Spiral-Like Paths on Triangulated Terrains

Martin Held, Stefan de Lorenzo
Department of Computer Science, University of Salzburg
[Jakob-Haringer-Straße 2, 5020 Salzburg, Austria]
held@cs.sbg.ac.at, slorenzo@cs.sbg.ac.at

In our previous work [1] we deal with the problem of covering a planar region R (bounded by straight-line segments and circular arcs) by moving a circular disk along a continuous path: The resulting spiral-like path starts in the interior of R and ends on its boundary, and is not self-intersecting. The fundamental geometric tool for our approach is the medial axis tree $\mathcal{T}_r^*(R)$, rooted at a point r, which is formed by a combination of a discretized version of the medial axis inside R and a set of so-called clearance lines. Imagine an impulse propagating through $\mathcal{T}_r^*(R)$ which moves from r towards the leaves of $\mathcal{T}_r^*(R)$. It is possible to produce a series of consecutive wavefronts by halting this impulse at fixed points in time. The final spiral-like path consists of several laps, where one lap is a portion of the spiral that winds around r exactly once. Each lap forms a polygonal chain. Initially, the first lap L_1 and the last lap L_m are computed by interpolating between successive wavefronts. The remaining, intermediate laps are created by interpolating between L_1 and L_m, see Figure 1a. In several practical applications it is important that the minimum distance from every a point on a lap to its next inner and outer lap is bounded by a user-specified distance $\Delta \in \mathbb{R}^+$. E.g., in a machining application this so-called step-over distance allows to control the material removal rate and to avoid excessive tool wear.

In the remainder of this abstract we outline ongoing work on a generalization of this path-generation strategy to spiral-like paths over piecewise-linear terrains in three dimensions. We will show that, once we have found a suitable substitute for the two-dimensional medial axis tree, the concept of impulse propagation as well as the interpolation procedure can be extended to this 3D setting. A sample spiral-like path on a simple terrain is shown in Figures 1b and 1c.

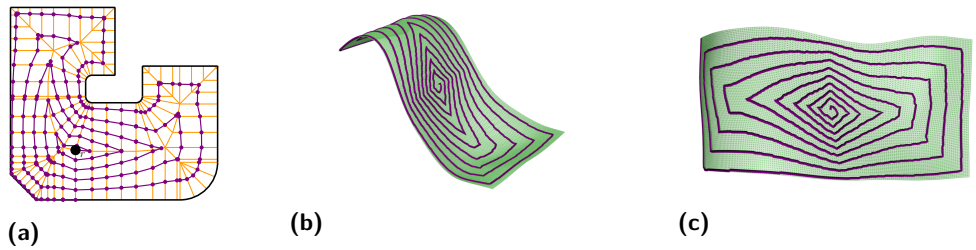

Figure 1 (a) A basic spiral-like path (highlighted in purple) inside a planar region R is defined by a series of corners which are situated on the discrete medial axis tree $\mathcal{T}_r^*(R)$ (highlighted in orange). (b–c) A spiral-like path (highlighted in purple) on a triangulated terrain.

We emphasize that naïvely mapping a 2D spiral-like path onto a terrain will result in a path that lacks any distance control between neighboring laps, for every meaningful interpretation of "distance" on a terrain. However, devices (e.g., a metal detector) or humans and animals (e.g., a rescue dog) that move along such a path should be expected to have a limited range of operation. Typical distance measures that we might be interested in are the geodesic distance or the line-of-sight distance. In the sequel we explain how to compute a coverage path $\mathcal{S}(P, \Delta)$ for a given triangulated terrain P and relative to a user-defined step-over $\Delta \in \mathbb{R}^+$ such that a geodesic disk of radius Δ covers P completely when it is moved along $\mathcal{S}(P, \Delta)$. The structure of choice in our generalized approach is the geodesic Voronoi

diagram of points on a triangulated terrain. It can be defined similarly to the standard Voronoi diagram of points in the plane by replacing the Euclidean norm with the geodesic metric.

Let P be a triangulated terrain. We place point sites along the polygonal boundary ∂P of P such that a roughly uniform spacing is achieved. The resulting geodesic Voronoi diagram $\mathcal{GVD}(P)$ forms a tree $\mathcal{T}_r(P)$ rooted at a point $r \in \mathcal{GVD}(P)$, where r is height-balanced (see [2] for further details). We will refer to a path along $\mathcal{T}_r(P)$ from r to a leaf of $\mathcal{T}_r(P)$ as a source branch, with source branches of maximal length being called radial paths. It is assumed that the order of these source branches is defined by the sequence in which the corresponding leaves appear when ∂P is traversed counter-clockwise. If p and q are two points on $\mathcal{T}_r(P)$, then the (geodesic) length $\ell(p, q)$ corresponds to the length of the unique path from p to q along $\mathcal{T}_r(P)$. The geodesic height of a point p is defined by $h(p) := \max_q \ell(p, q)$, where the maximum is taken over all nodes q of the sub-tree(s) of $\mathcal{T}_r(P)$ rooted at p. Now imagine an impulse propagating through $\mathcal{T}_r(P)$ which starts at r at time $t = 0$, splits at the nodes of $\mathcal{T}_r(P)$, and discharges simultaneously at the leaves at time $t = 1$. The impulse reaches a specific point p on the radial paths of $\mathcal{T}_r(P)$ at the activation time $t_p = \frac{h(r)-h(p)}{h(r)}$. This observation can be used to assign an activation time to every point on $\mathcal{T}_r(P)$ by recursively "peeling off" the corresponding radial paths. Due to space considerations, we refer to [1] for a more detailed description of this process in the 2D setting. As time progresses the impulse covers an increasing portion of $\mathcal{T}_r(P)$. Therefore, we can construct a series of $m + 1$ uniformly spaced wavefronts by defining a uniform decomposition of time. Each wavefront is given by a series of vertices (in which the first and last vertex coincide) that are situated on consecutive source branches. These wavefronts have to be chosen carefully such that the (symmetric) Hausdorff distance $H(w_i, w_{i+1})$, under the geodesic metric, between two neighboring wavefronts w_i and w_{i+1}, with $i \in \{0, 1, ..., m - 1\}$, is bounded by Δ.

The final spiral-like path $\mathcal{S}(P, \Delta)$ consists of a series m laps $L_1, L_2, ..., L_m$. Each lap is defined by a sequence of vertices which, again, lie on the source branches. Initially, two laps are computed. The first lap L_1 is generated by gradually moving its vertices from the corresponding vertices of w_0 (i.e. r) towards the vertices of w_1 along the consecutive source branches. Similarly, the last lap L_m is created by interpolating between w_{m-1} and w_m (i.e. ∂P). Every vertex of L_1 (or L_m) is at most Δ away from r (or ∂P). (Recall that the construction of the wavefronts ensures that w_1 is at most Δ away from r and the distance between w_{m-1} and ∂P is also bounded by Δ.) To construct to remaining laps $L_2, L_3, ..., L_{m-1}$, a modified impulse is used. This time it starts at the vertices of L_1, moves along $\mathcal{T}_r(P)$, and discharges concurrently at the vertices of L_m. The vertices of the lap L_{i+1} are produced by halting this modified impulse at $t = \frac{i}{m-2}$, with $i \in \{1, 2, ..., m - 2\}$. These laps $L_2, L_3, ..., L_{m-1}$ split the paths from the vertices of L_1 towards the respective vertices of L_m (along $\mathcal{T}_r(P)$) into $m - 1$ portions with a length of at most Δ.

This construction ensures that the maximum geodesic distance between neighboring wavefronts obeys the user-specified step-over Δ. We can also establish this property for specific vertices of the spiral-like path, and are investigating how to extend our distance considerations such that Δ is guaranteed to be respected along the entire path. We note that restricting our attention to a convex terrain does not seem to make the analysis any simpler.

References

1 Martin Held and Stefan de Lorenzo. On the Generation of Spiral-Like Paths Within Planar Shapes. *Journal of Computational Design and Engineering*, 2018, to appear.

2 Martin Held and Christian Spielberger. Improved Spiral High-Speed Machining of Multiply-Connected Pockets. *Computer-Aided Design and Applications*, 11(3):346–357, 2014.